Analytical Biochemistry 414 (2011) 154–162

Contents lists available at ScienceDirect

Analytical Biochemistry

journal homepage: www.elsevier.com/locate/yabio

Development of fluorescent substrates for microsomal epoxide hydrolase and application to inhibition studies

Christophe Morisseau [a,*], Maud Bernay [a], Aurélie Escaich [a], James R. Sanborn [a], Jozsef Lango [b], Bruce D. Hammock [a]

[a] Department of Entomology and Cancer Center, University of California – Davis, Davis, CA 95616, USA
[b] Department of Molecular Biosciences, University of California – Davis, Davis, CA 95616, USA

ARTICLE INFO

Article history:
Received 18 January 2011
Received in revised form 23 February 2011
Accepted 25 February 2011
Available online 1 March 2011

Keywords:
Microsomal epoxide hydrolase
Fluorescent substrate
α-Cyanocarbonate
Xenobiotic metabolism

ABSTRACT

The microsomal epoxide hydrolase (mEH) plays a significant role in the metabolism of numerous xenobiotics. In addition, it has a potential role in sexual development and bile acid transport, and it is associated with a number of diseases such as emphysema, spontaneous abortion, eclampsia, and several forms of cancer. Toward developing chemical tools to study the biological role of mEH, we designed and synthesized a series of absorbent and fluorescent substrates. The highest activity for both rat and human mEH was obtained with the fluorescent substrate cyano(6-methoxy-naphthalen-2-yl)methyl glycidyl carbonate (**11**). An in vitro inhibition assay using this substrate ranked a series of known inhibitors similarly to the assay that used radioactive *cis*-stilbene oxide but with a greater discrimination between inhibitors. These results demonstrate that the new fluorescence-based assay is a useful tool for the discovery of structure–activity relationships among mEH inhibitors. Furthermore, this substrate could also be used for the screening chemical library with high accuracy and with a Z' value of approximately 0.7. This new assay permits a significant decrease in labor and cost and also offers the advantage of a continuous readout. However, it should not be used with crude enzyme preparations due to interfering reactions.

The microsomal epoxide hydrolase (mEH,[1] EC 3.3.2.9) catalyzes the hydrolysis of epoxides or arene oxides to their corresponding diols [1,2]. It is a key hepatic enzyme involved in the metabolism of numerous xenobiotics such as the epoxides of 1,3-butadiene, styrene, naphthalene, benzo(α)pyrene, phenantoin, and carbamazepine [3–7]. The mEH is also involved in the extrahepatic metabolism of these agents [8,9]. Whereas for most compounds mEH action is a detoxification process [3–5], in some cases (e.g., for benzo(α)pyrene 4,5-oxide) diol formation can lead to the stabilization of a secondary epoxide, thereby increasing the mutagenicities and carcinogenicities of the product [10,11]. In addition, the role of mEH in xenobiotic detoxification is further supported by recent polymorphism studies showing a relationship between this enzyme and susceptibility to emphysema [12–14] and several forms of cancer [15–18].

Despite the fact that mEH knockout mice do not present an obvious phenotype [11], there are several new lines of evidence suggesting an endogenous role for this enzyme in addition to xenobiotic metabolism. A potential role of mEH in sexual development is supported by the fact that androstene oxide is a very good mEH substrate [19] and that mEH is an apparent subunit of the anti-estrogen-binding site [20]. Such a role could be related to the observed relation between mEH polymorphism and spontaneous abortion [21] or preeclampsia [22]. Furthermore, mEH is well expressed in follicle cells in the ovaries [23,24], and its expression is regulated by progesterone during the menstrual cycle [25]. Alternatively, over the past decade, mEH was also described as mediating the transport of bile acid in the liver [26,27]. The mechanism by which mEH participates in this transport is not known. Finally, mEH was recently suggested [28] to play a complementary role to soluble epoxide hydrolase (sEH) in the metabolism in the brain of naturally occurring epoxyeicosatrienoic acids, which are lipid mediators that have positive effects on cardiovascular disease, pain, and cancer treatment [29–31]. Obtaining potent mEH inhibitors will provide new tools to better understand the multiple roles of this enzyme.

Over the past decade, we have developed more potent mEH inhibitors to study the biological roles of mEH [32,33].

* Corresponding author. Fax: +1 530 751 1537.
E-mail address: chmorisseau@ucdavis.edu (C. Morisseau).

[1] *Abbreviations used:* mEH, microsomal epoxide hydrolase; sEH, soluble epoxide hydrolase; [^{3}H]cSO, tritium-labeled *cis*-stilbene oxide; UV, ultraviolet; NMR, nuclear magnetic resonance; DMSO, dimethyl sulfoxide; TMS, tetramethylsilane; HPLC, high-performance liquid chromatography; oa–TOF, orthogonal acceleration time-of-flight; ES, electrospray; ppm, parts per million; TLC, thin layer chromatography; BSA, bovine serum albumin; S/N, signal-to-noise; HTS, high-throughput screening; S/B, signal-to-background.

0003-2697/$ - see front matter © 2011 Elsevier Inc. All rights reserved.
doi:10.1016/j.ab.2011.02.038

Traditionally, tritium-labeled *cis*-stilbene oxide ([^{3}H]*c*SO) was used as substrate to measure inhibitor potency. Although this assay allows the discrimination of the most potent inhibitors, it has the disadvantages of being time-consuming and costly and of generating radiochemical waste. Therefore, with the need for testing numerous possible mEH inhibitors, it is necessary to investigate alternative assay strategies. Compared with radioactive and chromatographic-based assays, spectroscopic assays have the advantages of being straightforward in design and execution. With a few exceptions [34], a diol and its parent epoxide have similar spectral properties. Thus, after hydrolysis of an epoxide by an EH, an additional mechanism is usually required to generate an optical signal. To date, there are two methods described in the literature. The first one is based on the oxidative cleavage by periodate of the formed diol to yield an aldehyde with absorbent or fluorescent properties [35–37]. Although this method detects EH activity effectively, it generally requires a high concentration of substrate (mM range) and a high amount of diol formed (μM to mM range) and relies on external chemical modification steps. An alternate strategy based on intramolecular cyclization following diol formation to release an alcohol couple with suitable chromophores or fluorophores was developed in our laboratory for sEH assays [38,39]. These substrates are highly sensitive and relatively stable and show large changes in their ultraviolet (UV) and fluorescence spectra on hydrolysis. However, the compounds described to date for this latter approach are not good mEH substrates. Thus, here we report novel absorbent and fluorescent substrates for mEH. Furthermore, we optimize a kinetic assay for evaluating the potency of novel inhibitors and an endpoint assay for the screening of chemical libraries.

Materials and methods

Reagents

All reagents and solvents were purchased from Sigma–Aldrich (St. Louis, MO, USA) or Fisher Scientific (Pittsburgh, PA, USA), unless otherwise noted, and were used without further purification. 6-Methoxy-2-naphthaldehyde was obtained from TCI Chemicals (Portland, OR, USA). 2-Hydroxy-2-(2-methoxynaphthalen-6-yl)-acetonitrile was synthesized as described previously [40]. The inhibitors 2-nonylsulfanyl-propionamide (**A**), elaidamide (**B**), and 12-hydroxy-octadecanamide (**C**) were prepared previously in the laboratory [32,33]. Melting points were measured with a Thomas–Hoover apparatus (A. H. Thomas, Philadelphia, PA, USA) and are uncorrected. ^{1}H nuclear magnetic resonance (NMR) spectra were recorded on a Varian Mercury 300 (Walnut Creek, CA, USA) in d_6-dimethyl sulfoxide (DMSO) using tetramethylsilane (TMS) as an internal reference. High-performance liquid chromatography (HPLC) analyses were performed on a Waters Alliance 2795 HPLC system (Bedford, MA, USA) equipped with a Waters Symmetry C18 column (5 μm, 4.6 × 150 mm) and a UV–visible signal detection Waters 996 PDA detector operated in the wavelength range of 210 to 500 nm. Elution was performed at a flow rate of 0.4 ml/min with a gradient over 60 min from 100% solvent A (H_2O/acetonitrile/formic acid, 94.5:5:0.5) to 100% solvent B (acetonitrile/formic acid, 99.5:0.5). Accurate mass measurements were performed on a Micromass LCT, an orthogonal acceleration time-of-flight (oa–TOF) mass spectrometer configured with dual sprayer electrospray ion source, a standard Z-spray electrospray (ES), and lock-spray ionization sources operated in alternating polarity mode (Waters, Manchester, UK). Molecular ions of leucine enkephalin (cat. no. L9133, Sigma–Aldrich) at *m*/*z* 556.2771 Da in positive mode and *m*/*z* 554.2615 Da in negative mode were used to obtain accurate masses via the standard AMM procedure using MassLynx software (Waters, Manchester, UK).

Synthesis

Substrate and inhibitor structures are given in tables, and boldface numbers throughout the text refer to these compounds. The fluorescent substrates used in this study were synthesized as shown in Scheme 1. All substrates were synthesized as racemic mixtures, and compounds **2**, **4,** and **5** were prepared as *cis*/*trans* mixtures. NMR signals are reported in parts per million (ppm, δ) relative to TMS. For brevity, representative synthetic procedures are listed below. For additional synthetic procedures and spectral characterization, refer to Table S1 in the accompanying supplementary information.

*4-Nitrophenyl (oxiran-2-yl)methyl carbonate (**6**)*

To 370 mg of glycidol (5 mmol) dissolved in 10 ml of chilled dry dichloromethane, 1.0 g of 4-nitrophenylchloroformate (5 mmol) was added. Then 680 mg of triethylamine (5 mmol) was added slowly. The reaction was allowed to stir at 0 °C for 15 min and then warmed to room temperature and stirred for an additional 2 h. The reaction was washed with water until the aqueous phase was colorless. The organic phase was then washed with brine and dried over $MgSO_4$, filtered, and evaporated. The residue was purified by chromatography on SiO_2 to give 0.62 g (yield 50%) of the product (elution with 15% ethyl acetate in hexanes) as a yellowish powder. This product yielded a single spot on silica thin layer chromatography (TLC) (4:1 hexane/ethyl acetate solvent system). Melting point 41 to 43 °C. HRMS (*m*/*z*): $C_{10}H_{10}NO_6$ $[M+H]^+$ calcd: 240.0508 Da; found: 240.0502 Da. ^{1}H NMR (d_6-DMSO, TMS): δ 8.33 (D, J = 9.1 Hz, 2H), 7.59 (d, J = 9.3 Hz, 2H), 4.63 (dd, J = 4.1 Hz, 1H), 4.04 (dd, J = 4.0 Hz, 1H), 3.33 (m, 1H), 2.85 (d, J = 5.0 Hz, 1H), 2.72 (d, J = 5 Hz, 1H) ppm.

*Cyano(6-methoxynaphthalen-2-yl)methyl (oxiran-2-ylmethyl) carbonate (**11**)*

To 106 mg (0.5 mmol) of 2-hydroxy-2-(6-methoxynaphthalen-2-yl)acetonitrile, 120 mg of 4-nitrophenyl (oxiran-2-yl)methyl carbonate (**6**) (0.5 mmol) was added in chilled anhydrous tetrahydrofuran (2 ml). Then 4-dimethylaminopyridine (6 mg) was added. The reaction was allowed to stir at 0 °C for 15 min and then warmed to room temperature and stirred for 2 days. Ethyl acetate (5 ml) was added to the reaction. The organic layer was washed with aqueous K_2CO_3 until the aqueous layer was colorless. The organic layer was dried over $MgSO_4$, filtered, and evaporated. The residue was purified by chromatography on SiO_2 to give 110 mg (yield 73%) of the product (elution with 30% ethyl acetate in hexanes) as a white powder. This product yielded a single spot on silica TLC (4:1 hexane/ethyl acetate solvent system). Melting point 72 to 74 °C. HRMS (*m*/*z*): $C_{17}H_{16}NO_5$ $[M+H]^+$ calcd: 314.1028 Da; found: 314.1049 Da; m_{theoric} for $C_{34}H_{31}N_2O_{10}$ $[2M+H]^+$: 627.1979 Da; m_{found}: 627.1981 Da. ^{1}H NMR (d_6-DMSO, TMS): δ 8.10 (s, 1H), 7.95 (dd, J = 8.7 Hz, 2H), 7.63 (d, J = 11.6 Hz, 1H), 7.40 (s, 1H),7.24 (dd, J = 8.7 Hz, 1H), 6.80 (s, 1H), 4.57 (m, 1H), 4.00 (m, 1H), 3.89 (s, 3H), 3.28 (m, 1H),2.80 (t, J = 4.5 Hz, 1H), 2.66 (dd, J = 2.7 Hz, 1H) ppm.

Enzyme preparation

Recombinant rat mEH and human mEH were produced in a polyhedron positive baculovirus expression system and were partially purified as described previously [33]. This purification method allows the recovery of 20 mg of protein per liter of culture (40–60% yield in activity) with at least a 10-fold increase in purity. No esterase or glutathione transferase activities, which can interfere with EH assays, were detected in the purified enzyme preparations [40]. The enzyme preparations were kept at 4 °C until use, and no significant loss of activity was observed over a 3-month

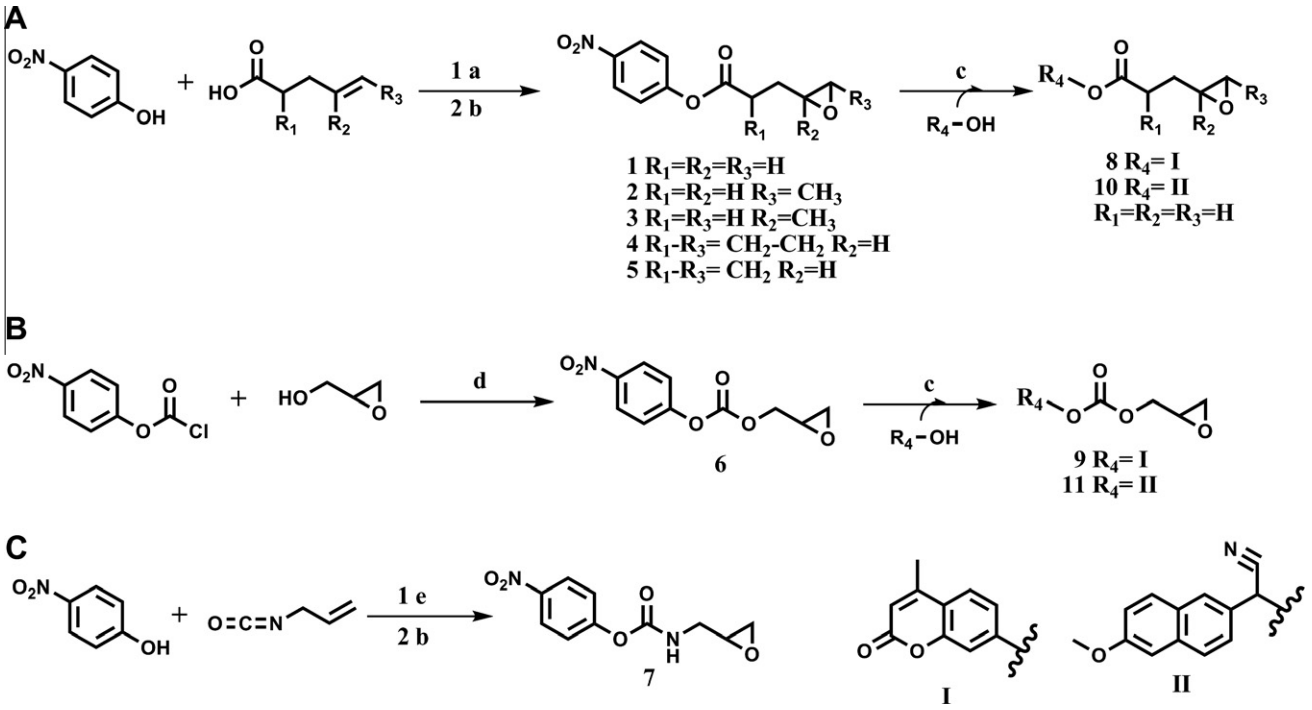

Scheme 1. Synthetic routes for the synthesis of A ester, B carbonate, and C carbamate substrates used in this study. Reagents and conditions: (a) 1-ethyl-3-(3-dimethylaminoprospyl) carboximide (EDC) 1.1 eq., triethylamine (TEA) 1 eq., 4-dimethylaminopyridine (DMAP) 0.1 eq., CH_2Cl_2, room temperature (RT) overnight; (b) *meta*-chloroperbenzoic acid (mCPBA) 1.3 eq., 1:1 CH_2Cl_2/sodium phosphate buffer (0.5 M, pH 7.4), RT overnight; (c) DMAP 0.1 eq., tetrahydrofuran (THF), RT overnight; (d) DMAP 0.1 eq., CH_2Cl_2, RT 2 h; (e) CH_2Cl_2, RT 2 h.

period in these conditions. Protein concentration was quantified by using the Pierce bisinchoninic acid (BCA) assay using fraction V bovine serum albumin (BSA) as the calibrating standard.

Standard curves

To convert the measured absorbance (in optical density) or fluorescence (in relative fluorescence units) signals into a molar basis, we used appropriate calibration curves. Stock solution of fluorophores and chromophore at 5 mM in DMSO were prepared. Serial dilution was then prepared in DMSO. In clear (for the chromophores) or black (for the fluorophores) polystyrene 96-well plates (Greiner Bio-One, Longwood, FL, USA), 2 μl of these diluted solutions (pure DMSO was used for the control wells) was added to 8 wells containing 198 μl of Tris–HCl buffer (100 mM, pH 9.0) with 0.1 mg/ml BSA (final volume 200 μl with 1% DMSO). Absorbance of 4-nitrophenol (for compounds **1–7**) was measured at 450 nm on a SpectraMax M2 (Molecular Devices, Sunnyvale, CA, USA) at 37 °C. Fluorescence of 7-hydroxy-4-methylcoumarin (for compounds **8** and **9**) and 6-methoxy-2-naphthaldehyde (for compounds **10** and **11**) was measured with excitation wavelengths of 355 and 330 nm, respectively, and emission wavelengths of 450 and 465 nm, respectively. Calibration curves for these three compounds contained at least six points from 0.005 to 0.5 μM with good linearity ($r^2 > 0.99$) in all cases.

Activity measurement

For the purification of mEH, and to serve as reference substrate, activity was determined using [^{3}H]*c*SO as described previously [33]. To 100 μl of diluted enzyme ($0.5 < [\text{protein}]_{\text{final}} < 16$ μg/ml) in Tris–HCl buffer (100 mM, pH 9.0) containing 0.1 mg/ml BSA, 1 μl of stock substrate solution was added ($[S]_{\text{final}} = 50$ μM). The mixture was incubated at 30 °C. After 5 min, the reaction was quenched by the addition of 250 μl of isooctane, which extracts the remaining epoxide from the aqueous phase. The activity was followed by quantifying the radioactive diol formed in the aqueous phase using a liquid scintillation counter (TriCarb 2810 TR, Perkin-Elmer, Downer Grove, IL, USA). Assays were performed in triplicate.

The specific activities for the novel substrates prepared were measured in clear (for compounds **1–7**) or black (for compounds **8–11**) polystyrene 96-well plates. In each well, 170 μl of diluted enzyme ($0.5 < [E]_{\text{final}} < 80$ μg/ml) in Tris–HCL buffer (100 mM, pH 9.0) containing 0.1 mg/ml BSA was dispensed and incubated at 37 °C for 5 min. To measure the background hydrolysis, buffer was dispensed in the control wells. Thus, 30 μl of substrate working solution (prepared by mixing just before use 133 μl of substrate stock solution at 5 mM in DMSO and 1860 μl of buffer) was added to each well ($[S]_{\text{final}} = 50$ μM). The amount of product form was measured kinetically for 5 min using the absorbance (compounds **1–7**) or fluorescence (compounds **8–11**) mode with the wavelengths described above. Results are the averages ± standard deviations of eight replicates. Assays were run under conditions where product formation was linearly dependent both on the concentration of enzyme and on the time for the course of the assay.

Kinetic constants determination

These assays were performed as per the determination of specific enzyme activity (vide supra). Constant enzyme concentrations of recombinant mEH (rat: 5 μg/ml; human: 16 μg/ml) were tested for their activity with various substrate concentrations ($0 \leqslant [S]_{\text{final}} \leqslant 50$ μM) at 37 °C. Initial velocities of substrate turnover were plotted versus the corresponding substrate concentration (see Figs. S1 and S2 in supplementary material for examples of plot obtained). The kinetic constants (V_M and K_M) were calculated by nonlinear fitting of the Michaelis–Menten equation to the obtained results using SigmaPlot (version 11.0, Systat Software, Chicago, IL,

USA). Results are means ± standard deviations of three independent determinations of the kinetic constants.

Assay conditions optimization

To optimize the concentration of enzyme for the inhibition potency measurement assays, various concentrations of mEH ($0 \leqslant [E]_{final} \leqslant 10$ μg/ml) were incubated in Tris–HCl buffer (0.1 M, pH 9.0) containing 0.1 mg/ml BSA with 25 μM substrate **11** at 37 °C. Enzyme activity was monitored by measuring the appearance of 6-methoxy-2-naphthaldehyde as described above. To reduce the relative background hydrolysis, mEH (rat: 0.5 μg/ml; human: 1.6 μg/ml) was incubated with 25 μM substrate **11** in six different buffers and at two different temperatures (30 and 37 °C). Enzyme activity was monitored as described above for 10 min. Results are means ± standard deviations of three independent measurements.

Inhibition potency assay

The inhibition potency (IC_{50}) of three described mEH inhibitors [32,33] was measured with compound **11** as substrate and with [^{3}H]*c*SO as described previously [33] for comparison. In black 96-well plates, to 170 μl of human mEH (2.0 μg/ml) or rat mEH (0.6 μg/ml) in Tris–HCl buffer (100 mM, pH 8.5) containing 0.1 mg/ml BSA, 2 μl of the inhibitors in DMSO solution was added. The mixture was incubated for 5 min at 30 °C. Then 30 μl of a 167-μM solution of compound **11** in a 77:23 buffer/DMSO mixture ($[S]_{final}$ = 25 μM; $[E]_{final}$: human = 1.6 μg/ml, rat = 0.5 μg/ml; $0 \leqslant [I]_{final} \leqslant 200$ μM). The activity was monitored for 10 min at 30 °C by measuring the appearance of 6-methoxy-2-naphthaldehyde as described above. Assays were performed in triplicate. By definition, IC_{50} values are concentrations of inhibitor that reduce enzyme activity by 50%. IC_{50} values were determined by regression of at least six datum points located in the linear region of the curve, with a minimum of two data points on either side of the IC_{50} values. Results are means ± standard deviations of three separate runs, each in triplicate.

High-throughput screening assay

The screening of a small library of chemicals [41] was performed using compound **11** as substrate. To black 96-well plates containing 20 μl of 10× concentrated test–compound solutions in 99:1 buffer/DMSO, 150 μl of Tris–HCl buffer (100 mM, pH 8.5) containing 0.1 mg/ml BSA was added in wells A1 to D1 (these four wells served as background control, whereas wells E1 to H1 served as full activity control), and 150 μl of the enzymes diluted in the same buffer was added to the rest of the plate using our Miniprep robotic system (Tecan, Durham, NC, USA). The plate was then mixed and incubated at 30 °C for 5 min. Across the plate, 30 μl of a 167-μM solution of compound **11** in a 77:23 buffer/DMSO mixture was added quickly ($[S]_{final}$ = 25 μM; $[E]_{final}$: human = 1.6 μg/ml, rat = 0.5 μg/ml; $[I]_{final}$ = 10 μM). The plate was incubated at room temperature for 30 min in the dark. The amount of formed 6-methoxy-2-naphthaldehyde was then measured by fluorescence detection with an excitation wavelength of 330 nm and an emission wavelength of 465 nm. Results are duplicate averages.

Results and discussion

Design and synthesis

To follow the same mechanism of intramolecular cyclization as reported for sEH substrates NEPC, CMNPC, and PHOME [38,39,43], the carbonyl of an ester or a carbonate should be optimally 4 atoms away from the first carbon of the oxirane ring. This allows, on epoxide hydrolysis by an EH, one of the hydroxyl groups of the diol to attack on the carbonyl, resulting in the liberation of the alcohol part of the ester or carbonate such as 4-nitrophenol for NEPC or α-cyanohydrin for CMNPC and PHOME [38,39,43]. The latter α-cyanohydrin rapidly decomposes to the fluorescent 6-methoxy-2-naphthaldehyde. It is important to verify that the substrates used do not contain appreciable amounts of the reaction product. Even trace amounts of product would significantly increase the background of the assay and reduce its signal-to-noise (S/N) ratio. For simplicity in the synthesis, we first screened a series of substrates with a 4-nitrophenol as reporter (Table 1). Earlier studies suggested that the mammalian mEH prefers *mono*-and *cis*-disubstituted epoxides over *trans*- and *gem*-disubstituted epoxides, whereas tri- and tetrasubstituted epoxides acted as inhibitors [2]. Furthermore, cycloalkene oxides are slow turnover substrates for mEH [3]. Thus, we synthesized substrates with *mono*-substituted **1**, disubstituted **2** and **3**, and cyclic **4** and **5** epoxides. For simplicity, compounds **2**, **4,** and **5** were prepared as *cis*/*trans* mixtures, knowing that if they are useful substrates they could be separated by chromatography. Similarly, all of the substrates were synthesized as racemic mixtures. Second, we optimized the best substrates with a series of fluorescent leaving groups (Table 2). Although we were able to obtain compounds with coumarin **8** and **9** and α-cyanohydrin **10** and **11** leaving groups, we were not able to isolate fluorescein and resorufin derivatives in significant amounts. These compounds degraded on the silica used during flash chromatography purification.

Substrate selectivity

We first investigated the selectivity of the rat and human mEH for a series of substrates with 4-nitrophenol as reporter (Table 1). Because the activity of esterases could interfere with the assay by hydrolyzing these compounds, the recombinant mEH were partially purified [33]. The active fraction used did not contain any measurable esterase activity [40]. A simple turbidity test showed that all of the substrates have solubility above 50 μM under the assay conditions. Thus, a final substrate concentration of 50 μM, similar to the one described for mEH activity [32], was used. Furthermore, assays were performed at pH 9.0 (the reported optimal pH for mEH activity) and 37 °C. The background hydrolyses of all of the 4-nitrophenyl ester-containing substrates (**1–5**) are similar (Table 1), and they are an order of magnitude higher than the one reported for NEPC [38] at pH 7.4. Although the epoxide should be more stable at higher pH, on the one hand, one could expect the ester function to be less stable, on the other. When looking at the influence of substitution on the epoxide (**1–5**) on the activity of the enzymes, we obtained measurable activity only for the *mono*-substituted epoxide **1.** These results agree with previous studies showing that the mammalian mEH prefers *mono*-substituted epoxides [2]. Nevertheless, compound **1** yielded S/N ratios above 40 for both enzymes, reflecting a small variation in the reporter signal and, thus, the robustness of the assay. We also found Z' values above 0.60, indicating a good separation band between the enzymes and the background signal [42]. However, the relatively high background hydrolysis rate of compound **1** limits its use. To reduce chemical hydrolysis while maintaining enzymatic activity, we first replaced the ester function of **1** by a carbonate **6** and a carbamate **7** (Table 1). Whereas there was a small increase in stability (lower background hydrolysis) for the carbonate, the carbamate was twice as stable as the ester. Unfortunately, we obtained a small hydrolysis rate for compound **7** in the presence of both enzymes. This could simply reflect that **7** is not a good substrate for mEHs. Alternatively, the carbamate stability is such that the di-hydrodiol

Table 1
Background hydrolysis and specific activity of rat and human mEHs for a series of 4-nitrophenol-containing substrates.

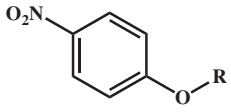		Background hydrolysis (nmol min^{-1})	Rat mEH				Human mEH			
			Specific activity (nmol min^{-1} mg^{-1})	S/B	S/N	Z'	Specific activity (nmol min^{-1} mg^{-1})	S/B	S/N	Z'
R: 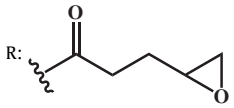	**1**	0.37 ± 0.02	23 ± 1	3	44	0.66	72 ± 7	4	68	0.64
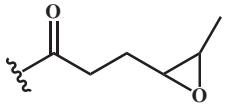	**2**	0.18 ± 0.01	<5	2	5	<0	<2	1	5	<0
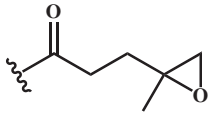	**3**	0.55 ± 0.11	<5	1	2	<0	<2	1	2	<0
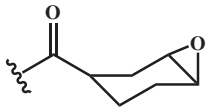	**4**	0.18 ± 0.01	<5	1	12	<0	<2	1	15	<0
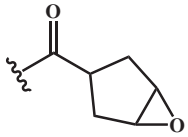	**5**	028 ± 0.04	<5	1	8	<0	<2	1	10	<0
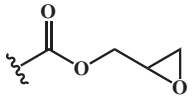	**6**	0.31 ± 0.02	29 ± 2	5	32	0.67	51 ± 2	3	53	0.82
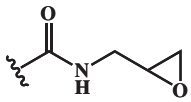	**7**	0.18 ± 0.04	<5	1	3	<0	<2	1	4	<0

Note. S/B, signal-to-background ratio; S/N, signal-to-noise ratio; Z', screening window coefficient [42].

Table 2
Background hydrolysis and specific activity of rat and human mEHs for a series of fluorescent substrates.

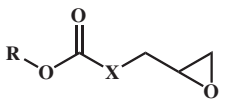			Background hydrolysis (nmol min^{-1})	Rat mEH				Human mEH			
				Specific activity (nmol min^{-1} mg^{-1})	S/B	S/N	Z'	Specific activity (nmol min^{-1} mg^{-1})	S/B	S/N	Z'
R	X										
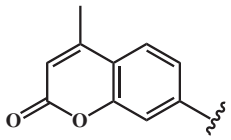	CH_2	**8**	0.014 ± 0.001	40 ± 2	4	102	0.76	17 ± 2	4	97	0.61
	O	**9**	0.016 ± 0.001	48 ± 4	4	62	0.67	21 ± 2	5	79	0.76
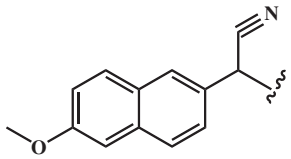	CH_2	**10**	0.011 ± 0.001	21 ± 2	3	67	0.62	12 ± 1	4	52	0.61
	O	**11**	0.018 ± 0.003	68 ± 4	5	48	0.73	25 ± 2	4	30	0.66

Note. S/B, signal-to-background ratio; S/N, signal-to-noise ratio; Z', screening window coefficient [42].

was not able to generate the chromophore rapidly enough and it became rate limiting. On the other hand, compound **6** was as good as compound **1** as substrate for the two enzymes tested.

To obtain more stable substrates so as to generate more sensitive assays, we followed a strategy used for sEH substrates [39]. We replaced the good leaving group 4-nitrophenol of compounds

1 and **6** with two less reactive fluorescent phenols (Table 2). The two umbeliferol derivatives (**8** and **9**) and the two cyanohydrin derivatives (**10** and **11**) have similar background hydrolyses that are an order of magnitude smaller than those of **1** and **6.** The rat mEH yielded specific activities twice as high for the fluorescent substrates (**8–11**) than for the absorbance-based substrates (**1** and **6**), whereas for the human mEH we obtained specific activities 2- to 6-fold smaller for **8** to **11** than for **1** and **6.** Nevertheless, all of the fluorescent substrates in Table 2 yielded S/N ratios above 40 for both enzymes, reflecting a small variation in the reporter signal and, thus, increased the robustness of the assay. We also found Z' values above 0.60, indicating that these substrates could be easily used in high-throughput screening (HTS) assays [42]. Although all four substrates gave good results, we concentrated on the carbonates (**9** and **11**) that gave higher specific activity than the corresponding esters (**8** and **10**).

To further characterize the new substrates, we determined the kinetic constants for compounds **9** and **11.** In addition, the K_M and V_M of *c*SO were also determined for comparison (Table 3). For the rat mEH, the *c*SO and **9** have similar K_M values, whereas that of **11** is one order of magnitude lower. On the other end, the V_M of *c*SO is 30 to 50% greater than of **9** and **11.** Finally, the specific constants (V_M/K_M) are similar for *c*SO and **9** and 10-fold greater for **11.** This indicates that for the rat mEH, **11** is a 10 times better substrate than the other substrates tested and is better than previously reported rat mEH substrates [2,3]. For the human mEH, we observed very high values for the kinetic constants of *c*SO. Because mEH has a two-step mechanism involving the formation and hydrolysis of a covalent intermediate [3], K_M in this case is not a measurement of the affinity of the substrate for the enzyme; rather, K_M reflects the concentration of substrate for which the velocity is half-maximal. The obtained K_M values should increase in parallel with the V_M values [44], as observed with the *c*SO for the human mEH. Whereas the K_M values of **9** and **11** were roughly 10- and 40-fold lower, respectively, than that for the *c*SO, their V_M values were also 15 to 30 times lower. Consequently, the specific constant (V_M/K_M) of **11** is 3 to 6 times larger than that of the other substrates tested, indicating that **11** overall is a better substrate for the human mEH. Furthermore, this substrate is hydrolyzed similarly as or faster than previously described human mEH substrates [2,4,37].

Assay optimization

The development of an assay to evaluate the potency of mEH inhibitors requires appropriate concentrations of substrate and enzyme. For **11,** a final substrate concentration of 25 μM was used, which is 10-fold above the K_M of both rat and human mEH and is below **11** maximal solubility in the buffer (~50 μM). The saturated substrate condition is advantageous because it provides stability to the assay and small variations in the substrate concentration will not affect the enzyme activity. The assay conditions can, of course, be optimized for different analytical goals. For example, the excess of substrate used here allows a longer assay time and minimizes the effect of small technical errors. In contrast, short assay times will increase analytical throughput. In effect, to measure inhibitor potency, a short assay (5–10 min) is preferable, whereas for a library of compound screening a longer incubation time (30–60 min) is preferred for automated assays. Thus, we tested the hydrolysis of **11** by various concentrations of the human mEH over 30 min (Fig. 1). For 10 min, we observed a linear appearance of the fluorescent aldehyde for [human mEH] up to 8 μg/ml. For 30 min, only [human mEH] below 3 μg/ml yielded a linear response. Therefore, we selected a human mEH concentration of 1.6 μg/ml that yields a signal-to-background (S/B) ratio of approximately 3, an S/N ratio of approximately 40, and a Z' value of 0.75. At this enzyme concentration, the appearance of the fluorescence was linear up to 60 min of incubation. Similar results (not shown) were obtained with the rat mEH. Optimal assay performances were obtained with a partially purified rat mEH concentration of 0.5 μg/ml.

As seen in Fig. 1, the background hydrolysis of **11** is still significant. To reduce the hydrolysis, we investigated the effect of temperature, pH, and buffer salts on the chemical and enzymatic hydrolysis of **11** (Fig. 2). As expected, reducing the incubation temperature from 37 to 30 °C decreased the catalytic activity of the human mEH by approximately 30% for all of the buffers tested (Fig. 2A). However, it also reduced the background hydrolysis by at least 50%, yielding larger S/B ratios at the lower temperature (Fig. 2B). For the three pH values tested, higher catalytic activities were obtained for the Tris–HCl buffers with little change in background hydrolysis among the buffers. Using these solutions, the enzymatic activity did not decrease significantly when the pH was reduced from 9.0 to 8.5 (as expected) [3], whereas the background hydrolysis was reduced by approximately 30%. Reducing the pH further to 8.0 resulted in a reduction of the enzyme activity by approximately 20%. Such reduction in activity was expected because mEH was previously shown to have an optimal pH around 9.0, and its activity quickly decreases as pH is decreased [1,3].

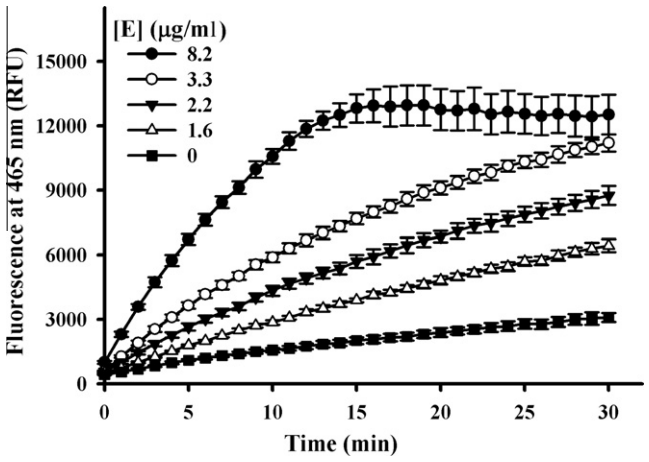

Fig.1. Time course hydrolysis of 25 μM compound **11** by various concentrations of human mEH in Tris–HCl buffer (100 mM, pH 9.0) containing 0.1 mg/ml BSA at 37 °C. Results are average ± standard deviations of eight replicates. RFU, relative fluorescence units.

Table 3
Kinetic constants for rat and human mEHs incubated in Tris–HCl buffer (100 mM, pH 9.0) containing 0.1 mg/ml BSA at 37 °C.

	Rat mEH			Human mEH		
	K_M (μM)	V_M (nmol min^{-1} mg^{-1})	V_M/K_M (nmol min^{-1} mg^{-1} μM^{-1})	K_M (μM)	V_M (nmol min^{-1} mg^{-1})	V_M/K_M (nmol min^{-1} mg^{-1} μM^{-1})
*c*SO	35 ± 3	115 ± 10	3.3 ± 0.4	141 ± 9	570 ± 40	4.0 ± 0.1
9	22 ± 3	61 ± 3	2.8 ± 0.2	12.0 ± 0.7	20 ± 1	1.7 ± 0.1
11	2.3 ± 0.4	89 ± 8	40 ± 7	3.8 ± 0.6	42 ± 3	11 ± 1

Note. Results are averages ± standard deviations of three independent measurements.

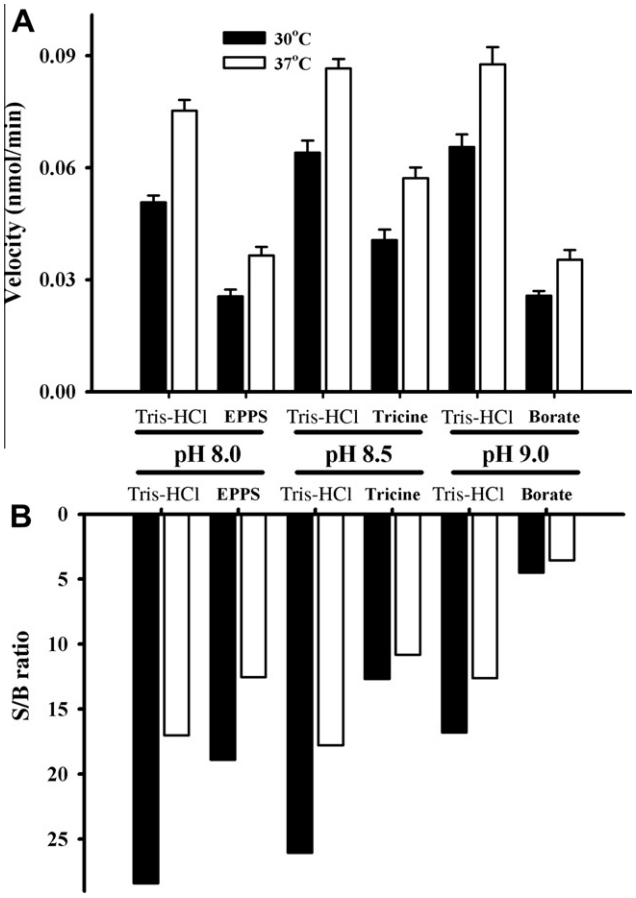

Fig.2. Effect of pH and temperature on the hydrolysis of 25 μM compound 11 by 1.6 μg/ml human mEH over a 10-min period: (A) velocities; (B) S/B ratios. All of the buffers contained 0.1 mg/ml BSA. Results are averages ± standard deviations of eight replicates. EPPS, *N*-2-hydroxyethylpiperazine propane sulfonic acid.

Because the background hydrolysis decreases by a similar amount, there is no advantage from lowering the pH from 8.5 to 8.0. Therefore, we measured activity in a Tris–HCl buffer at pH 8.5 and 30 °C. This yielded an S/B ratio >5, an S/N ratio >50, and a Z' value >0.8.

Inhibitor assays

To evaluate the effectiveness of this new assay, we determined the inhibition potency of three previously described rat mEH inhibitors [32,33]. In Table 4, we report the experimentally determined IC_{50} values using the fluorescent assay described here with compound **11** as substrate and with the standard *c*SO-based radiochemical assay for reference. Overall, similar results were obtained for the rat and human mEHs. The results obtained with the *c*SO are similar to the IC_{50} values published previously [32,33]. Although both assays gave the same relative pattern of inhibition, the IC_{50} values for each inhibitor are very different with each substrate. These data highlight that IC_{50} values are very dependent on the method of measurement, as shown previously for sEH inhibition [39]. The enzyme concentrations used for both assays were similar (rat mEH: 1.0 and 0.5 μg/ml for *c*SO and **11,** respectively; human mEH: 3.2 and 1.6 μg/ml for *c*SO and **11,** respectively), and the substrate concentrations were in the same range ([*c*SO] = 50 μM, [**11**] = 25 μM). However, relative to their respective K_M values (Table 3), these [S] values are quite different. The *c*SO concentration is near its K_M value for the rat enzyme and 3-fold below the K_M for the human mEH. Thus, for *c*SO, the assays are not run under saturation conditions. Therefore, it is easier to inhibit the enzyme, which yields smaller IC_{50} values. To illustrate this, using a concentration of **11** near its K_M ([**11**] = 2.5 μM), we obtained for the rat mEH an IC_{50} for inhibitor **A** of 0.5 μM, which is similar to the one obtained with *c*SO. For the results presented in Table 4, the concentration of substrate **11** is 5- to 10-fold above its K_M for both enzymes. Thus, the assays are run at saturation conditions, making it harder for an inhibitor to compete with the substrate to bind to the active site of the enzyme. These conditions result in larger IC_{50} values. Although the inhibitors appeared to be less potent (i.e., larger IC_{50} values), using compound **11** as substrate under the described conditions, the assay has the advantage of giving a better discrimination between potent inhibitors. For example, between inhibitors **A** and **C,** the *c*SO assay yielded only a 2- to 5-fold difference, whereas the fluorescent assay yielded more than a 30-fold difference. This makes it easier to interpret structure–activity data and, thus, simplifies the design of more potent inhibitors.

Finally, we tested the assay based on compound **11** as substrate to screen a small library of chemicals. We screened a library of

Table 4
Comparison of inhibition potencies (IC_{50}) for selected mEH inhibitors.

Inhibitor		Rat mEH		Human mEH	
		*c*SO	**11**	*c*SO	**11**
		IC_{50} (μM)			
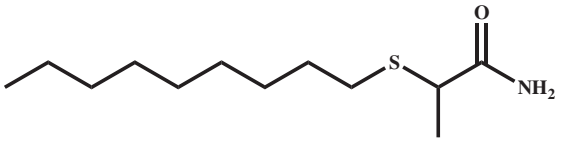	**A**	0.4 ± 0.1	4.2 ± 0.7	0.5 ± 0.1	6.0 ± 0.9
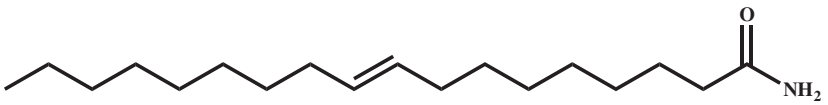	**B**	0.5 ± 0.1	63 ± 5.0	1.0 ± 0.1	140 ± 13
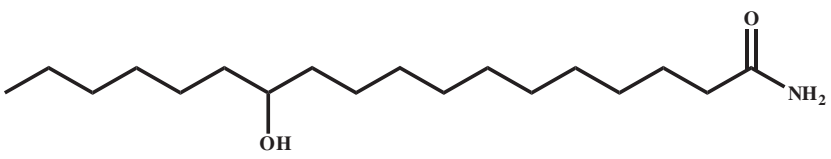	**C**	1.1 ± 0.1	123 ± 13	2.6 ± 0.3	>200

Note. Results are averages ± standard deviations of three independent measurements.

pesticides that we recently prepared [41] at a final concentration of 10 μM. Most HTS assays use endpoint measurement after a relatively long reaction time between the enzyme and substrate [43]. Thus, after the addition of the substrate, we incubated the enzymatic reactions for 30 min at room temperature before to detect the amount of formed 6-methoxy-2-naphthaldehyde as an endpoint measurement (see Table S2 in supplementary material). With these conditions, we obtained on average (n = 4 for each enzyme) S/B = 3.0 ± 0.3, S/N >30, and Z' = 0.69 ± 0.03. Between duplicates, we observed overall approximately 5% variation in mEH inhibition. These values showed that an assay using **11** as substrate is suitable for HTS. At a concentration of 10 μM, four compounds (pyrethrum, Asana, triclosan, and BDE47) showed significant inhibition of mEH from both species. When these four chemicals were retested with **11** in the inhibition potency assay method described above, we confirmed mEH inhibition at 10 μM. However, no inhibition was observed when *c*SO was used as a substrate, suggesting false-positive responses from the fluorescent assay.

To properly use the assay described here, one should be aware of a number of cautions. First, when preparing the compound, it is critical that the substrate not contain hydrolysis product that would significantly increase the background. These essays are very attractive for partially purified enzymes. However, traces of esterases, glutathione *S*-transferases, or other EH activity will lead to high background in the assay and difficulty in interpreting results. Thus, in situations where the competing enzymatic reactions cannot be easily inhibited or removed, radiochemical or chromatographic-based assays should be used. Certainly, these latter assays should be used to characterize novel tissue homogenate. Finally, the assay described here, like all fluorescence-based assays [41], is subject to interferences. This is a particular risk when inhibitors are used at high concentrations. It could, for example, quench the reporting signal by interfering with the excitation or emission photons. It may also form micelles that could sequester the substrate away from the enzyme. Such interferences were probably the source of the false-positive inhibition we obtained while screening a small chemical library (see above).

Conclusions

We have developed a fluorescent assay for mammalian mEH inhibition studies. We validated the use of this assay for measurement of the potency of mEH inhibitors as well as for HTS. The new fluorescent assay is a more powerful tool to investigate mEH inhibition than the costly and labor-intensive radioactive assays. Thus, cyano(6-methoxy-naphthalen-2-yl)methyl glycidyl carbonate (**11**) will be a very useful tool for the development of new mEH inhibitors that will further investigations into the biological role of mEH.

Acknowledgments

We thank Sung-Hee Hwang for his technical help in the structural characterization of the compounds synthesized here. This work was partially funded by National Institute of Environmental Health Services (NIEHS) Grants ES02710 and ES013933 and NIEHS Superfund Basic Research Program Grant P42 ES04699. B.D.H. is a George and Judy Marcus Senior Fellow of the American Asthma Foundation.

Appendix A. Supplementary data

Supplementary data associated with this article can be found, in the online version, at doi:10.1016/j.ab.2011.02.038.

References

[1] F. Oesch, Mammalian epoxide hydrases: inducible enzymes catalysing the inactivation of carcinogenic and cytotoxic metabolites derived from aromatic and olefinic compounds, Xenobiotica 3 (1973) 305–340.
[2] J.W. Newman, C. Morisseau, B.D. Hammock, Epoxide hydrolases: their roles and interactions with lipid metabolism, Prog. Lipid Res. 44 (2005) 1–51.
[3] B.D. Hammock, D. Grant, D. Storms, Epoxide hydrolase, in: F.P. Guengerich (Ed.), Comprehensive Toxicology, Biotransformation, vol. 3, Pergamon, Oxford, UK, 1997, pp. 283–305.
[4] A.J. Fretland, C.J. Omiecinski, Epoxide hydrolases: biochemistry and molecular biology, Chem. Biol. Interact. 129 (2000) 41–59.
[5] M. Decker, M. Arand, A. Cronin, Mammalian epoxide hydrolases in xenobiotic metabolism and signaling, Arch. Toxicol. 83 (2009) 297–318.
[6] H. Tan, Q. Wang, A. Wang, Y. Ye, N. Feng, X. Feng, L. Lu, W. Au, Y. Zheng, Z. Xia, Influence of GSTs, CYP2E1, and mEH polymorphisms on 1,3-butadiene-induced micronucleus frequency in Chinese workers, Toxicol. Appl. Pharmacol. 247 (2010) 198–203.
[7] G.P. Carlson, Metabolism and toxicity of styrene in microsomal epoxide hydrolase-deficient mice, J. Toxicol. Environ. Health A 73 (2010) 1689–1699.
[8] J. Zheng, M. Cho, P. Brennan, C. Chichester, A.R. Buckpitt, A.D. Jones, B.D. Hammock, Evidence for quinone metabolites of naphthalene covalently bound to sulfur nucleophiles of proteins of mouse Clara cell after exposure to naphthalene, Chem. Res. Toxicol. 10 (1997) 1008–1014.
[9] E. Teissier, S. Fennrich, N. Strazielle, J.-L. Daval, D. Ray, B. Schlosshauer, J.-F. Gershi-Egea, Drug metabolism in in vitro organotypic and cellular models of mammalian central nervous system: activities of membrane-bound epoxide hydrolase and NADPH–cytochrome P-450 (*c*) reductase, Neurotoxicology 19 (1998) 347–356.
[10] J. Szeliga, A. Dipple, DNA adducts formation by polycyclic aromatic hydrocarbon dihydrodiol epoxides, Chem. Res. Toxicol. 11 (1998) 1–11.
[11] M. Miyata, G. Kudo, Y.-H. Lee, T.J. Yang, H.V. Gelboin, P. Fernandez-Salguero, S. Kimura, F.J. Gonzalez, Targeted disruption of the microsomal epoxide hydrolase gene: microsomal epoxide hydrolase is required for the carcinogenic activity of 7,12-dimethylbenz[α]anthracene, J. Biol. Chem. 274 (1999) 23963–23968.
[12] C.A.D. Smith, D.J. Harrison, Association between polymorphism in gene for microsomal epoxide hydrolase and susceptibility to emphysema, Lancet 350 (1997) 630–633.
[13] D.L. DeMeo, C.P. Hersh, E.A. Hoffman, A.A. Litonjua, R. Lazarus, D. Sparrow, J.O. Benditt, G. Criner, B. Make, F.J. Martinez, P.D. Scanlon, F.C. Sciurba, J.P. Utz, J.J. Reilly, E.K. Silverman, Genetic determinants of emphysema distribution in the national emphysema treatment trial, Am. J. Respir. Crit. Care Med. 176 (2007) 42–48.
[14] P.J. Castaldi, C.P. Hersh, J.J. Reilly, E.K. Silverman, Genetic associations with hypoxemia and pulmonary arterial pressure in COPD, Chest 135 (2009) 737–744.
[15] C. Kiyohara, A. Otsu, T. Shirakawa, S. Fukuda, J.M. Hopkin, Genetic polymorphisms and lung cancer susceptibility: a review, Lung Cancer 37 (2002) 241–256.
[16] J. To-Figueras, M. Gené, J. Gómez-Catalán, E. Piqué, N. Borrego, M. Caballero, F. Cruellas, A. Raya, M. Dicenta, J. Corbella, Microsomal epoxide hydrolase and glutathione *S*-transferase polymorphisms in relation to laryngeal carcinoma risk, Cancer Lett. 187 (2002) 95–101.
[17] S.W. Baxter, D.Y.H. Choong, I.G. Campbell, Microsomal epoxide hydrolase polymorphism and susceptibility to ovarian cancer, Cancer Lett. 177 (2002) 75–81.
[18] M. Pande, C.I. Amos, C. Eng, M.L. Frazier, Interactions between cigarette smoking and selected polymorphisms in xenobiotic metabolizing enzymes in risk for colorectal cancer: a case-only analysis, Mol. Carcinog. 49 (2010) 974–980.
[19] U. Vogel-Bindel, P. Bentley, F. Oesch, Endogenous role of microsomal epoxide hydrolase: ontogenesis, induction, inhibition, tissue distribution, immunological behavior, and purification of microsomal epoxide hydrolase with 16α,17α-epoxyandrostene-3-one as substrate, Eur. J. Biochem. 126 (1982) 425–431.
[20] F. Mésange, M. Sebbar, B. Kedjouar, J. Capdevielle, J.-C. Guillemot, P. Ferrara, F. Bayard, F. Delarue, J.-C. Faye, M. Poirot, Microsomal epoxide hydrolase of rat liver is a subunit of the anti-oestrogen-binding site, Biochem. J. 334 (1998) 107–112.
[21] X. Wang, M. Wang, T. Niu, C. Chen, X. Xu, Microsomal epoxide hydrolase polymorphism and risk of spontaneous abortion, Epidemiology 9 (1998) 540–545.
[22] J. Laasanen, E.-L. Romppanen, M. Hiltunen, S. Helisalmi, A. Mannermaa, K. Punnonen, S. Heinonen, Two exonic single nucleotide polymorphisms in the microsomal epoxide hydrolase gene are jointly associated with preeclampsia, Eur. J. Hum. Genet. 10 (2002) 569–573.
[23] H. Mukhtar, R.M. Philpot, J.R. Bend, The postnatal development of microsomal epoxide hydrase, cytosolic glutathione *S*-transferase, and mitochondrial and microsomal cytochrome P-450 in adrenals and ovaries of female rats, Drugs Metab. Dispos. 6 (1978) 577–583.
[24] E.A. Cannady, C.A. Dyer, P.J. Christian, I.G. Sipes, P.B. Hoyer, Expression and activity of microsomal epoxide hydrolase in follicles isolated from mouse ovaries, Toxicol. Sci. 68 (2002) 24–31.

[25] S.L. Popp, I.S. Abele, M.B. Buck, M.B. Stope, L.J. Blok, P. Hanifi-Moghaddam, C.W. Burger, P. Fritz, C. Knabbe, Microsomal epoxide hydrolase expression in the endometrial uterine corpus is regulated by progesterone during the menstrual cycle, J. Mol. Histol. 41 (2010) 111–119.
[26] C. Alves, P. von Dippe, M. Amoui, D. Levy, Bile acid transport into hepatocyte smooth endoplasmic reticulum vesicles is mediated by microsomal epoxide hydrolase, a membrane protein exhibiting two distinct topological orientations, J. Biol. Chem. 268 (1993) 20148–20155.
[27] Q. Zhu, W. Xing, B. Qian, P. von Dippe, B.L. Shneider, V.L. Fox, D. Levy, Inhibition of human *m*-epoxide hydrolase gene expression in a case of hypercholanemia, Biochem. Biophys. Acta 1638 (2003) 208–216.
[28] A. Marowsky, J. Burgener, J.R. Falck, J.M. Fritschy, M. Arand, Distribution of soluble and microsomal epoxide hydrolase in the mouse brain and its contribution to cerebral epoxyeicosatrienoic acid metabolism, Neuroscience 163 (2009) 646–661.
[29] J.D. Imig, B.D. Hammock, Soluble epoxide hydrolase as a therapeutic target for cardiovascular diseases, Nat. Rev. Drug Discov. 8 (2009) 794–805.
[30] B. Inceoglu, K.R. Schmelzer, C. Morisseau, S.L. Jinks, B.D. Hammock, Soluble epoxide hydrolase inhibition reveals novel biological functions of epoxyeicosatrienoic acids (EETs), Prostaglandins Other Lipid Mediat. 82 (2007) 42–49.
[31] D. Panigrahy, A. Kaipainen, E.R. Greene, S. Huang, Cytochrome P450-derived eicosanoids: the neglected pathway in cancer, Cancer Metastasis Rev. 29 (2010) 723–735.
[32] C. Morisseau, J.W. Newman, D.L. Dowdy, M.H. Goodrow, B.D. Hammock, Inhibition of microsomal epoxide hydrolases by ureas, amides, and amines, Chem. Res. Toxicol. 14 (2001) 409–415.
[33] C. Morisseau, J.W. Newman, C.E. Wheelock, T. Hill III, D. Morin, A.R. Buckpitt, B.D. Hammock, Development of metabolically stable inhibitors of mammalian microsomal epoxide hydrolase, Chem. Res. Toxicol. 21 (2008) 951–957.
[34] R.N. Wixtrom, B.D. Hammock, Continuous spectrophotometric assays for cytosolic epoxide hydrolase, Anal. Biochem. 174 (1988) 291–299.
[35] C. Mateo, A. Archelas, R. Furstoss, A spectrophotometric assay for measuring and detecting an epoxide hydrolase activity, Anal. Biochem. 314 (2003) 135–141.
[36] K. Doderer, R.D. Schmid, Fluorometric assay for determining epoxide hydrolase activity, Biotechnol. Lett. 26 (2004) 835–839.
[37] W. Shen, J. Zhang, G. Mao, K. Jiang, Q. Zhu, A long-wavelength, fluorogenic probe for epoxide hydrolase: 7-(2-(oxiran-2-yl)ethoxy) resorufin, Biol. Pharm. Bull. 32 (2009) 1496–1499.
[38] E.C. Dietze, E. Kuwano, B.D. Hammock, Spectrophotometric substrates for cytosolic epoxide hydrolase, Anal. Biochem. 216 (1994) 176–187.
[39] P.D. Jones, N.M. Wolf, C. Morisseau, P. Whetstone, B. Hock, B.D. Hammock, Fluorescent substrates for soluble epoxide hydrolase and application to inhibition studies, Anal. Biochem. 343 (2005) 66–75.
[40] G. Shan, B.D. Hammock, Development of sensitive esterase assays based on α-cyano-containing esters, Anal. Biochem. 299 (2001) 54–62.
[41] C. Morisseau, O. Merzlikin, A. Lin, G. He, W. Feng, I. Padilla, M.S. Denison, I.N. Pessah, B.D. Hammock, Toxicology in the fast lane: application of high-throughput bioassays to detect modulation of key enzymes and receptors, Environ. Health Perspect. 117 (2009) 1867–1872.
[42] J.H. Zhang, T.D. Chung, K.R. Oldenburg, A simple statistical parameter for use in evaluation and validation of high throughput screening assays, J. Biomol. Screen. 4 (1999) 67–73.
[43] N.M. Wolf, C. Morisseau, P.D. Jones, B. Hock, B.D. Hammock, Development of a high throughput screen for soluble epoxide hydrolase inhibition, Anal. Biochem. 355 (2006) 71–80.
[44] I.H. Segel, Enzyme Kinetics: Behavior and Analysis of Rapid Equilibrium and Steady-State Enzyme Systems, John Wiley, New York, 1993.